

## Powder Processing Science and Technology for Increased Reliability

Fred F. Lange\*

Materials Department, College of Engineering,  
University of California, Santa Barbara, California 93106

Issues concerning powder consolidation methods compatible with the colloidal approach and issues associated with other powder processing steps, viz., densification and microstructural control, are presented with regard to research directions leading to more reliable ceramics. [Key words: powder, microscopy, colloidal chemistry, processing, heterogeneity.]

### I. Introduction

With their multiplicity of elemental combinations and crystal structures, ceramics exhibit unique properties that are still being uncovered. Ceramics are needed to implement many technology scenarios ranging from advanced heat engines to transmission of information.

Ceramic-processing technology has advanced little beyond the needs of functional ceramics. Traditional ceramic processing inherently lacks a clear approach for controlling microstructure heterogeneities and microstructure uniformity. Property variability and, thus, ambiguous engineering reliability stem from uncontrolled microstructures. Engineering reliability is a matter of processing reliability.

Most forming methods are generally unacceptable for ceramics. Their brittle nature precludes deformation methods commonly used for metals. Melt casting produces friable ceramics because of, in part, uncontrolled grain growth during solidification. Some advanced ceramics,

viz.,  $\text{Si}_3\text{N}_4$  and  $\text{SiC}$ , decompose prior to melting. Glass-ceramic processing, a special melt-forming method that takes advantage of Newtonian rheology to form shapes and crystallization after solidification to control microstructure, produces nonequilibrium phase assemblages and is limited to glass-forming chemistries. Columnar grain growth and uneconomical deposition rates are disadvantages for chemistries that can be shaped by vapor condensation methods. Liquid precursor methods, e.g., sol-gel processing, suffer from large volume changes during fluid removal, pyrolysis, and/or densification, which limits this method to shaping small bodies, i.e., particles, thin films, and fibers. Most advanced ceramics are formed as powder compacts made dense by heat treatment. Although powder processing is a many-bodied problem prone to heterogeneities and nonuniform phase distributions, it is the most efficient method to form ceramics. The objective of this article is to review new approaches and thinking leading to the increased reliability of ceramics processed with powders.

### II. Heterogeneities Common to Powder Processing

Powder processing involves four basic steps: (1) powder manufacture, (2) powder preparation for consolidation, (3) consolidation to an engineering shape, and (4) densification/microstructural development that eliminates void space and produces the microstructure that optimizes properties. Each step has the potential for introducing a detrimental heterogeneity which will either persist during further processing or develop into a new heterogeneity during densification and microstructural development.

Because the number of heterogeneities per unit volume can be small, they are best observed with an experiment sensi-



Dr. Lange is professor in the Depts. of Materials and Chemical and Nuclear Engineering at the University of California, Santa Barbara. He received a B.S. in ceramic science from Rutgers University in 1961 and a Ph.D. in solid state technology from Pennsylvania State University in 1965. After graduate studies, he spent two years in a postdoctoral capacity at the Atomic Energy Research Establishment, Harwell, England. During 1967-76 he was with Westinghouse Research and Development Labs, and during 1976-86 he was with Rockwell Int'l Science Center.

A Fellow of the ACerS, he is affiliated with the Basic Science Division. In 1982 he was a recipient of the Society's Ross Coffin Purdy Award and in 1987 he presented the Basic Science Division's Sosman Lecture.

Manuscript No. 199141. Received September 26, 1988; approved October 20, 1988.

Presented at the 89th Annual Meeting of the American Ceramic Society, Pittsburgh, PA, April 29, 1987 (Paper No. 199-B-87 (Sosman Lecture)).

Supported in part by the U.S. Air Force Office of Scientific Research under Contract No. AFOSR-87-0291.

\*Member, American Ceramic Society.

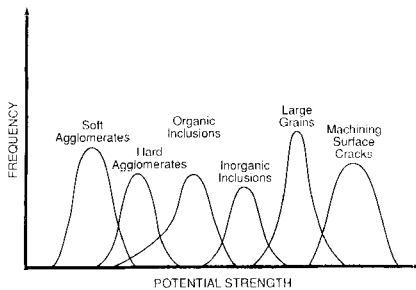


Fig. 1. Schematic plot of frequency versus potential strength of different flaw populations potentially present in a ceramic material. Frequency distribution and ordering depends on processing method and material characteristics.

tive to heterogeneities. Because strength is sensitive to stress concentrators, microstructural heterogeneities that are stress concentrators can be best observed by fracture and examination of fracture origins.\* As schematically illustrated in Fig. 1, many different heterogeneities may coexist. Each can be viewed as a strength-limiting flaw population, introduced during some stage of processing. The ordering of the common flaw populations shown in Fig. 1 and their strength-size distribution depends on the material and its processing. For example, some materials, such as SiC and  $\beta$ -Al<sub>2</sub>O<sub>3</sub>, are prone to develop a microstructure containing large, platelike grains. These platelike grains can be the first flaw population uncovered during strength determinations, whereas some other flaw population, e.g., cracklike voids produced by the differential shrinkage of agglomerates, can be the dominant heterogeneity observed either in the same materials processed in a different manner or in other materials not prone to abnormal grain growth. Once the dominant flaw population is identified and eliminated by processing changes, another flaw population with a higher mean strength will be uncovered. Its strength-size distribution will now dominate strength statistics. The processor interested in eliminating heterogeneities must first identify the dominant heterogeneity observed at fracture origins, ascertain how this heterogeneity is introduced during processing, and then make the appropriate processing changes to eliminate the heterogeneity. This is an iterative scheme.

Many microstructural heterogeneities stem from the powder itself. Agglomerates are a major heterogeneity in powders. The attractive interparticle forces responsible for free particle agglomeration include van der Waals and capillary forces. Capillary forces are produced when water vapor condenses at particle contacts. After a liquid has been removed by evaporation, particles can be cemented together with previously soluble salts (e.g., with hydroxides) left at contact positions. Most ceramic powders are manufactured by decomposing and/or reacting a precursor at moderate temperatures. Nanometer-size crystallites, formed during pyrolysis,

sinter together to a continuous low-density crystallite network. When the pyrolyzed material is milled to make particles, the resulting particles can be partially dense, sintered crystallites, i.e., very strong agglomerates.

Current consolidation technology is based on dry pressing and requires flowable powders to uniformly fill a die cavity. Particles within dry powders are held together by van der Waals forces. Flowable powders require large particles because the separating force produced by differential acceleration during flow is proportional to particle mass. Because the separating forces produced by the micrometer-sized particles desired for ceramic processing are insufficient to overcome attractive (e.g., van der Waals) forces, ceramic powder slurries containing polymer additions are spray dried to purposely form large (>50  $\mu$ m) agglomerates and a flowable powder.

Agglomerates with different bulk densities can persist during powder consolidation to form cracklike voids during densification because of their different shrinkage rates relative to the surrounding powder compact.<sup>3</sup> Agglomerates purposely produced by spray drying may not uniformly deform to fill interagglomerate void space<sup>4</sup> during consolidation. They will leave irregular voids that persist after densification. Agglomerates also limit densification.<sup>5,6</sup>

Powders contain organic and inorganic inclusions introduced by both the manufacturer and the processor during powder preparation for consolidation. Some of these heterogeneities are introduced when powders are milled to reduce the size of hard agglomerates and/or are exposed to the environment. Organic inclusions disappear during densification to leave irregularly shaped voids.<sup>7</sup> Inorganic inclusions can react with the powder during densification and/or produce microcracks during either cooling from the densification temperature or subsequent stressing. Clean rooms are ineffective because the manufacturer supplies the inclusions with the powder.

Postdensification hot-gas isopressing can eliminate some voids that remain after pressureless densification.<sup>8</sup> Recent results strongly suggest that void closure occurs by deformation,<sup>9</sup> and cracklike voids, e.g., those produced by the differential shrinkage of agglomerates, are the first to close.<sup>10</sup> Unfortunately, postdensification hot-gas isopressing cannot eliminate pores that intersect the surface and other heterogeneities, e.g., inclusions. Moreover, postdensification hot-gas isopressing can exaggerate the size of voids just beneath the surface when the ligament separating the void from the surface punctures by deformation.<sup>9</sup>

Many advanced ceramics contain more than one phase and are produced by mixing two or more powders prior to consoli-

\*The strength of several ceramics can be relatively insensitive to flaw size and thus insensitive to flaws introduced during processing. These ceramics include optimally aged transformation-toughened ZrO<sub>2</sub><sup>1</sup> and certain fiber composites with very weak fiber-matrix interfacial bond strengths.<sup>2</sup> These relatively few ceramics possess a toughening mechanism that increases the resistance of the material to crack growth, i.e., the critical stress intensity factor, as the crack grows. Unfortunately, these special toughening mechanisms are currently limited to certain material systems and temperatures, but, when fully exploited, they could result in structural ceramics that are relatively insensitive to flaw populations introduced during processing and thus produce a material with a relatively narrow strength distribution, i.e., high Weibull modulus.

dation and densification. As discussed later in this paper, a second phase can be used to eliminate abnormally large grains which are common heterogeneities developed during densification of noncubic crystalline structures. Phase homogeneity is a major issue in these multiphase ceramics, and even when the desired homogeneity is obtained during mixing, heterogeneities can arise if mass segregation occurs by sedimentation after mixing.

If reliable ceramics are to be produced, methodologies must be developed to ensure, with a high probability, that heterogeneities will be eliminated from powders and that they will not be reintroduced in subsequent processing steps. As discussed in the next section, the colloidal approach has this potential.

### III. Colloidal Approach

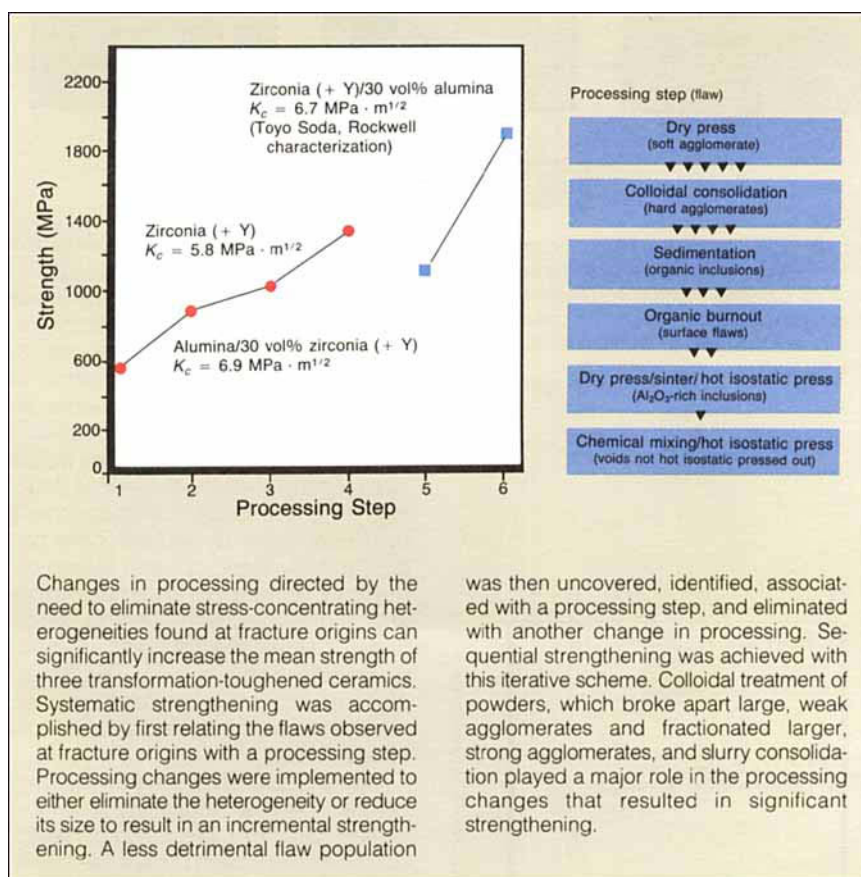
Heterogeneities must be separated from current powders. When technologies are developed to produce powders free of heterogeneities, we must have a methodology available to process these powders without introducing new heterogeneities. Powders must flow to fill either die cavities or molds to consolidate shapes. Once a powder is fractionated and made flowable, it cannot be exposed to an uncontrolled environment prior to consolidation. As will be come evident, the colloidal approach is consistent with these requirements.

Many of the heterogeneities discussed earlier in this paper can be eliminated from their sources, i.e., the powders, by manipulating and controlling interparticle forces as practiced in colloid science. Certain aspects of colloidal processing require repulsive interparticle forces, whereas others require attractive forces. Powders disperse to form a system of separated particles when repulsive forces dominate and they floc to form a low-density network of touching particles when attractive forces dominate. Repulsive interparticle forces are used to break apart weak agglomerates, fractionate inclusions greater than a given size, and mix different fractionated powders. Once fractionated and mixed, the interparticle forces can be made attractive to form a low-density, deformable network that prevents mass segregation.

Slurry rheology depends on interparticle forces and particle volume fraction.<sup>11-12</sup> Dilute, dispersed slurries exhibit Newtonian rheology (viscosities independent of shear rate). At high volume fractions, the slurries become dilatant (viscosity increases with shear rate) because the system must increase its volume to allow closely spaced, repulsive particles to slip past one another. Flocced slurries exhibit pseudoplastic, thixotropic rheology (viscosity decreases with increasing shear rate and history-dependent viscosity) because the applied forces separating attractive particles depend on differential

acceleration (shear rate). Once separated, flocculation and network formation are time dependent. Pourable, dispersed slurries can contain up to 60 vol% solids, whereas the volume fraction of pourable, flocced slurries is much lower (between 5 and 20 vol%) and depends on the particle mass (size), which governs the forces separating particles during flow.

A number of fundamental interactions can be used to alter interparticle forces.<sup>13</sup> These forces include attractive van der Waals forces, repulsive electrostatic forces, attractive or repulsive steric forces, and attractive capillary forces. With the exception of van der Waals forces, the manipulation of interparticle forces usually requires the addition of a surface-active agent to a liquid-particle system. Electrostatic repulsive forces develop when solute ions



are attracted to or dissociated from particle surfaces to produce a system of similarly charged particles. Steric forces are developed by macromolecules that attach themselves to the surface of the particle. Charged macromolecules, i.e., polyelectrolytes, can produce both repulsive electrostatic and steric forces. Although the science of interparticle forces has a strong theoretical base verified through direct surface force measurements,<sup>13</sup> the choice of the best surface-active agent used to control interparticle forces is still a matter of trial and error for most ceramic systems.

Figure 2 illustrates one colloidal approach to treat and store ceramic powders

prior to consolidation.<sup>7</sup> As-received, dry powders are dispersed in an appropriate fluid with a surfactant that produces interparticle repulsive forces. These repulsive forces keep particles separated once shearing forces break apart weak agglomerates. Partially sintered and other strong agglomerates which cannot be broken apart and inorganic inclusions

mixed-particle network which prevents phase separation during storage and further processing.

The effect of interparticle forces on mass segregation due to sedimentation was investigated<sup>14</sup> by centrifuging both dispersed and flocced slurries containing a mixture of  $\text{Al}_2\text{O}_3$  and  $\text{ZrO}_2$  (30 vol%) powders colloiddally treated and mixed as described earlier in this paper.<sup>†</sup> The centrifuged masses were dried, densified and sectioned to examine phase distribution by scanning electron microscopy (SEM), using energy dispersion X-ray analysis (EDX). Figure 3 illustrates the Zr/Al count ratio versus the normalized distance from the bottom to the top of the sintered, centrifuged mass. As shown, this ratio was nearly constant ( $\pm 3\%$ ) across the specimen prepared from the flocced mixture and equal to that of the initial composited mixture. As expected, the dispersed slurry produced different results. First, although the Zr/Al count ratio was nearly constant ( $\pm 13\%$ ) across  $\approx 90\%$  of the normalized specimen thickness, it significantly increased near the top of the specimen. Second, the average Zr/Al count ratio corresponded to only  $\approx 14$  vol%  $\text{ZrO}_2$ ; many of the smaller, less-massive  $\text{ZrO}_2$  particles were left behind in the centrifuged supernatant. In addition, as shown in Fig. 4, larger particles of both phases were observed at the bottom of the specimen and smaller particles at the top. Similar observations showed that both the phase distribution and the size of each phase was uniform throughout the specimen prepared from the flocced slurry. These results clearly show that the touching particle network within a flocced slurry can prevent mass segregation due to sedimentation.

The question concerning mixed-phase uniformity and what tools can be used to define its uniformity has recently been addressed.<sup>15</sup> The method is simple and can be related to the slurry rheology,<sup>16</sup> and it has the potential to access mixing uniformity during processing as a nondestructive evaluation tool.

When a multiphase body is observed by SEM, the X-rays collected produce an EDX spectrum that quantitatively defines the atomic fraction of each element. If different elements are associated with different phases, the content of each phase within the area scanned can be determined. At low magnifications, the EDX spectrum defines the fraction of each phase within the large body. With reasonable counting periods, the standard deviation for different areas examined at low magnifications is low (usually  $<3\%$ ) and associated with counting statistics. At very high magnifications, the area examined may not be representative of the large body; e.g., the scanned area may only cover one of the many phases, and the deviation of the spectrum, relative to the large body, can be very large. At some

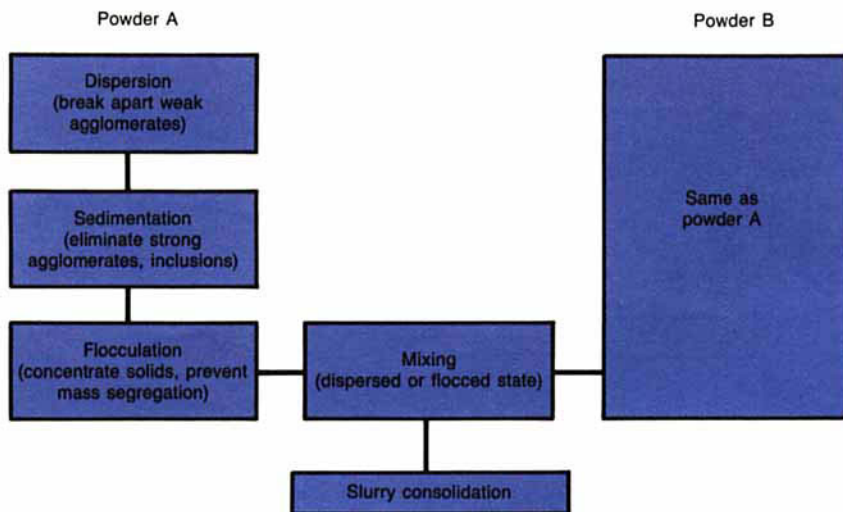


Fig. 2. One colloidal method for breaking apart weak agglomerates and fractionating desired particles from unwanted hard agglomerates and inclusions. Each powder in a multiphase system is treated the same before mixing.<sup>7</sup>

greater than a given size are eliminated by sedimentation. This step can be accelerated by centrifuging. After the undesired larger particles, strong agglomerates, and inclusions are removed, the retained dispersed slurry containing the desired particles is flocced by changing the interparticle forces from repulsion to attraction. Floccing concentrates the particles to form a weak, continuous, touching network which consolidates under its own weight, partially separating the particles from the liquid phase. Flocced slurries can be washed to remove excess salts and/or surfactants. Centrifuging can further concentrate this particle network. As discussed later in this paper, floccing also prevents mass segregation during storage even when acted upon by centrifugal forces.

Figure 2 also shows that two or more powder phases, separately treated as summarized in the preceding paragraph, can be mixed to form multiphase slurries. If the different slurries are colloiddally compatible, i.e., do not floc one another, they can be redispersed (by again adding the proper surface agent) and mixed. More commonly, the phases are not colloiddally compatible. These systems can still be mixed because flocced mixtures can be mechanically redispersed by a device that produces a high shear-rate field (an ultrasonic horn, high-speed rotor, etc.). As the mechanically dispersed mixture leaves the high shear-rate field, it flocs to form a new

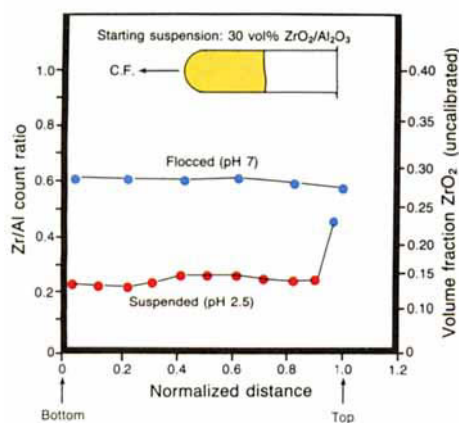


Fig. 3. Zr/Al count ratio (obtained from an EDX spectra) versus the normalized distance detailing the  $\text{ZrO}_2$  and  $\text{Al}_2\text{O}_3$  distribution for mixed powder slurries centrifuged in the dispersed and flocced states.

<sup>†</sup>Both  $\text{Al}_2\text{O}_3$  and  $\text{ZrO}_2$  can be dispersed at pH 2 and are colloiddally compatible when mixed, i.e., they remain dispersed. Both can be flocced at pH 8.

intermediate magnification, the standard deviation will begin to depart from that produced by counting statistics. At this magnification, the area scanned is statistically identical (within an acceptable standard deviation somewhat larger than that due to counting statistics) with the large body. The size of this area thus defines the smallest area that contains the same phase distribution as the whole body. This area ( $A_U$ ) can be defined quantitatively and used to represent phase uniformity. The better the mixing, the smaller  $A_U$ .  $A_U$  is an extrinsic property of the multiphase material that depends on processing.<sup>15</sup>

Values of  $A_U$  can be related to different mixing methods and mixing periods, e.g., different resident periods for mixed slurries within a high shear rate field, and to the properties of the mixed slurry itself. Lange and Miller<sup>16</sup> have shown that  $A_U$  can be related to the viscosity of flocced, two-phase slurries, and they have suggested that an in-line viscosity measurement could be used to determine phase uniformity (defined by a number, i.e.,  $A_U$ ) during processing.

#### IV. Consolidation from the Slurry State

Once colloidally treated, powders should not be dried. Slurries contain soluble salts, produced, e.g., by a reaction with the powder itself, which can bond touching particles when the last bit of liquid evaporates from their pendular ring. That is, agglomerates, previously eliminated by colloidal treatment, will reform during drying. Drying also reexposes the particles to uncontrolled environments which can reintroduce inclusions. Colloidally treated slurries could be piped directly to a consolidation machine.

A major issue for exploiting the colloidal approach is to directly form powder compacts from the slurry state. Two conventional slurry consolidation methods, slip casting and tape casting, can be directly used with colloidally prepared powders, and, with some innovative changes, injection molding could be adapted to do the same. Each of these conventional forming methods is limited, e.g., slip casting best produces thin-walled bodies, and a large amount of polymer must be removed after injection molding. For these reasons, investigators are exploring alternative slurry-shaping methods where either the solid/liquid ratio remains constant during shaping, i.e., slurry molding, or the particles are partially partitioned from the liquid during shaping, e.g., pressure filtration.

To avoid excessive shrinkage during fluid removal and/or densification, molding methods require slurries containing the highest possible fraction of particles. Molding also requires flow. As detailed by Aksay and co-workers,<sup>17</sup> pourable ceramic slurries containing in excess of 60 vol% of particulates require highly repulsive interparticle forces. In addition, they have

also shown that the volume fraction of particulates can be further increased with the proper particulate-size distribution.<sup>18</sup> As shown in Fig. 5, the addition of a given fraction of finer particulates decreases the slurry viscosity.

Once molded, the rheological properties of the slurry must be dramatically altered to allow shape retention during unmolding. This change can be induced by a variety of different phenomena that include freezing (used in injection molding), gelation,<sup>19</sup> and in situ flocculation. Each can change a flowable slurry into a firm body without fluid-phase removal. Rheological changes are not without problems; they can produce strain gradients. For example, volume changes can accompany freezing, and freezing initiates at the surface. In addition, if capillary pressure arises during fluid removal, bodies molded with dispersed slurries will shrink unless an attractive, touching-particle network is formed first (e.g., by in situ flocculation). Shrinkage and expansion gradients can lead to significant stresses and/or disruptive phenomena. The potential problem of mass and phase segregation produced by sedimentation within a highly filled, moldable dispersed slurry needs further study.

Moldable slurries can also be achieved when flocced bodies are rapidly sheared. Forces produced by differential accelerations break apart the attractive particle network to produce Newtonian rheology; the network reforms shortly after the shear field is removed. Firm, fully saturated bodies containing between 50 and 60 vol% particulates can be produced by either centrifuging<sup>14</sup> or pressure filtering<sup>20</sup> lower viscosity, flocced slurries. When these firm bodies are coupled to high-intensity ultrasound, they fluidize to fill a cavity. Once the ultrasound is removed, the rheology of the slurry quickly reverts to a firm, molded body. The author's experience with this innovative molding method suggests that attenuation of the ultrasound is one problem that must be addressed.

Pressure filtration produces a fully saturated powder compact as particles within a slurry are partitioned as liquid flows through a filter leaving particles behind to form a consolidated layer. Hard ferrite particles within a slurry can be aligned with a magnetic field prior to consolidation. Pressure filtration is used to form ceramic magnets with a variety of applications because the desired/permanent magnetic field is produced during consolidation.<sup>21</sup> With the development of moldable casting dies made of a porous plastic material, an innovative pressure filtration machine has recently been introduced<sup>22</sup> that enables the rapid production of large, relatively complex shaped bodies. Although these new filter presses are currently marketed to produce functional articles (from plates to sinks) with traditional clay-based slurries, they represent the first

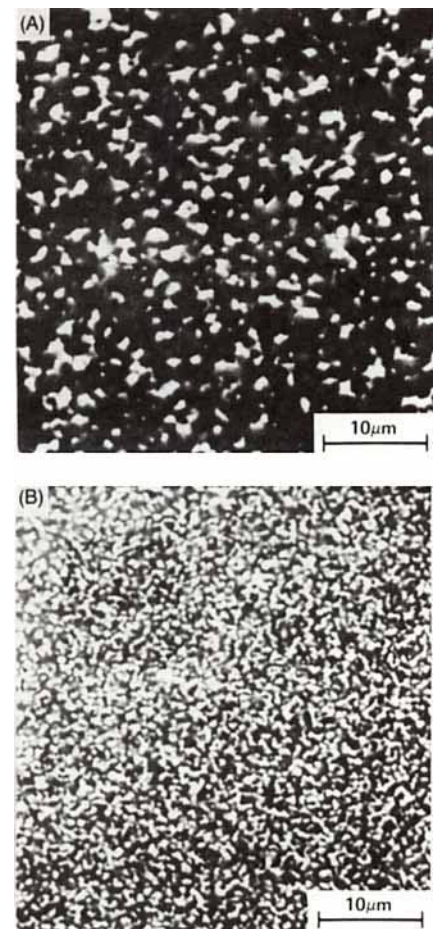


Fig. 4. Micrographs of dense,  $\text{Al}_2\text{O}_3\text{-ZrO}_2$  composite ceramic formed by centrifuging a dispersed slurry, illustrating particle-size and phase distributions at the (A) bottom and (B) top of the specimen.

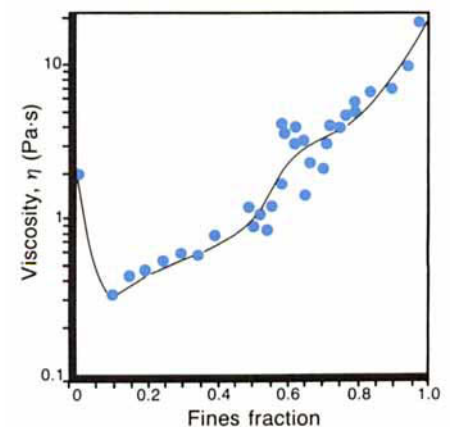


Fig. 5. Viscosity (extrapolated to zero shear rate) versus fine fraction for  $\text{Al}_2\text{O}_3$  (0.55 volume fraction) slurries, dispersed with a polyelectrolyte, containing coarse ( $0.8 \mu\text{m}$ ) and fine ( $0.2 \mu\text{m}$ ) powders.<sup>18</sup>

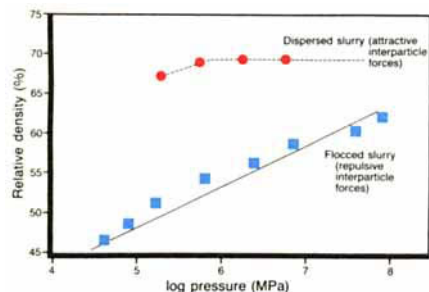


Fig. 6. Relative density of different bodies produced from the same  $\text{Al}_2\text{O}_3$  powder by filtration at different applied pressures. Bodies were consolidated from either dispersed (pH 2) or flocced (pH 8) aqueous slurries containing 20 vol% solids.

generation of machines to form advanced components with advanced ceramics. It has also been demonstrated that pressure filtration can also be conducted under conditions of isopressure,<sup>20</sup> which decreases the probability of disruptive phenomena occurring by die constraint during pressure release. In addition, with innovative design, pressure filtration offers the advantage that after consolidation, much of the liquid can be removed with a high-pressure gas, i.e., through invasion percolation, before the body is removed from the molding die.

The kinetics of pressure filtration obeys Darcy's differential equation<sup>23</sup> for fluid flow through porous media, which, when integrated with the appropriate boundary conditions, shows that the thickness of the consolidated layer ( $h$ ) formed under constant pressure ( $P$ ) is parabolically related to time ( $t$ ) by

$$t = h^2 \frac{u}{2kP} \left( \frac{v_f - v_0}{v_0} \right) \quad (1)$$

where  $u$  is the liquid viscosity and  $v_0$  and  $v_f$  are the volume fractions of particulates within the slurry and consolidated layer, respectively. The permeability ( $k$ ) is inversely related to the resistance of fluid flow through the consolidated layer. Assuming that the particles are identical spheres with diameter  $d$ , one can estimate the permeability of a consolidated layer with the Kozeny-Carman relation, which models the layer as a bundle of tortuous capillary tubes with hydraulic diameters resembling slits.<sup>2</sup>

$$k = \frac{d^2(1 - v_f)^3}{36cv_f^2} \quad (2)$$

where the Kozeny constant ( $c$ ) defines the shape and tortuosity of the flow channels ( $c = 5$  for many systems).

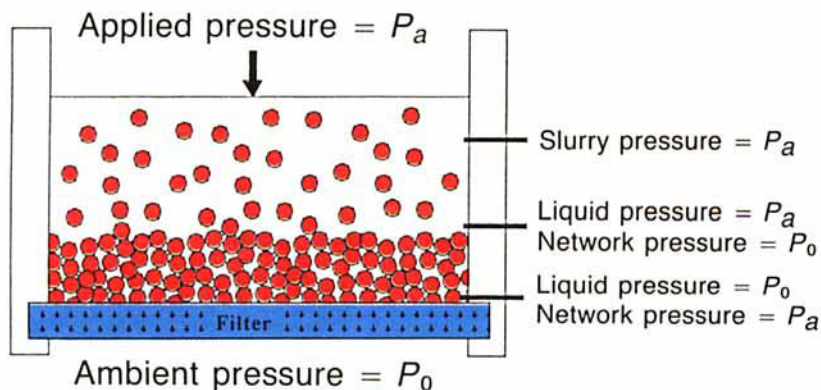


Fig. 7. Schematic of pressure distribution during pressure filtration showing that a pressure gradient exists within the network of consolidated particles.

The mechanics of particle packing during filtration and the mechanics of pressure-filtered bodies have been examined for aqueous slurries containing  $\text{Al}_2\text{O}_3$  powder with a mean diameter of approximately  $0.6 \mu\text{m}$ .<sup>20</sup> The electrostatic method (pH control) was used to produce either dispersed or flocced slurries. Figure 6 shows the relative density of consolidat-

ed bodies after filtration is complete, as plotted against the logarithm of the applied pressure. Consistent with observations by Fennelly and Reed,<sup>25</sup> the highest packing density is achieved with dispersed slurries. Also, the packing density achieved with dispersed slurries is pressure independent for pressures  $>0.5 \text{ MPa}$ . Figure 6 shows that the packing of consolidated layers from flocced slurries is very pressure sensitive and appears to obey a consolidation law (relative density linearly related to the logarithm of pressure) similar to dry powders.

The mechanics of particle packing during pressure filtration can be explained with the aid of Fig. 7, which schematically describes the pressure distribution within the filtration system. Assuming that the particles have not formed a continuous network (the case of a dispersed slurry), the slurry pressure is identical with the fluid pressure and equal to the pressure ( $P_a$ ) exerted by the plunger. Ambient, atmospheric pressure  $P_0$  exists on the external side of the filter. The differential pressure across the filter and consolidated layer ( $P_a - P_0$ ) is the driving force for fluid flow. A gradient in fluid pressure exists across the consolidated layer; i.e., at the slurry-layer interface,  $P_f = P_a$ , and, neglecting the pressure gradient across the filter,  $P_f = P_0$  at the filter-layer interface. Because the total pressure within the consolidated layer must be equal to the applied pressure, the particle network must support a pressure gradient equal, but opposite, to the fluid pressure. That is, at the filter-layer interface, the network pressure,  $P_n = P_a$ , and, at the slurry-layer interface,  $P_n = 0$ . Because network pressure will produce particle rearrangement, during filtration, the packing density will be greatest at the filter-layer interface and decrease to the layer-slurry interface. Once the plunger meets the consolidation layer, filtration will continue until the differential fluid pressure dissipates; i.e., the fluid pressure decreases to ambient pressure. During this period, the gradient in the network pressure dissipates to the applied pressure to produce a uniform particle-packing density across the consolidation layer.

With the information presented in the preceding paragraph and Fig. 6, note that, during pressure filtration, flocced slurries produce large gradients in packing density relative to dispersed slurries. For this case, there is no clear demarcation between the slurry and the consolidated layer as there is for dispersed slurries.

The mechanics of particle packing have only been addressed with static models,<sup>26</sup> which does not address particle rearrangement. Why dispersed slurries produce high packing densities at very low pressures has not yet been detailed, but it must be related to the effect of repulsive interparticle forces on rearrangement.

It is rarely recognized in ceramic tech-

nology that powders exhibit nonlinear elastic stress-strain behavior similar to that described by Hertz<sup>27</sup> when spheres are pressed together. Walton<sup>28</sup> has reported that the compressive stress-strain response of a powder can be expressed as  $\sigma = B\varepsilon^{3/2}$ , where  $B$  depends on the relative density of the powder compact (average number of contacts per particle) and the elastic properties of the particles and is independent of particle size. Figure 8(A) describes this response for  $\text{Al}_2\text{O}_3$  powder compacts as determined with strain recovery measurements after pressure filtration of both flocced and dispersed slurries.<sup>20</sup> As illustrated, relatively small stresses produce large strains and the compact becomes stiffer as the stress is increased. It is not the porosity that produces this behavior, but the large displacements between particle centers when a "point" contact is elastically compressed into an area contact. Thus, after a powder has been consolidated and the pressure has been released, large elastic strains are recovered and the compact grows.

The greater the consolidation pressure, the greater the recoverable strain. Inclusions within the powder which are either stiffer (e.g., dense agglomerates, whiskers, or fibers) or more compliant (organic inclusions) will store less or more strain relative to the powder compact, respectively, during consolidation. Figure 8(A) also illustrates that the elastic response of a dense  $\text{Al}_2\text{O}_3$  inclusion ( $E = 400$  GPa) and a very compliant polymer inclusion ( $E = 1$  GPa). The differential strain relieved by the inclusion relative to the powder will produce detrimental stresses during strain recovery. Likewise, the powder compact can be damaged by metal die cavities which constrain the strain recovery of powders pressed within them.

For consolidated dry powders, strain recovery is nearly instantaneous with pressure release. As shown in Fig. 8(B), the strain recovery for compacts produced by pressure filtration is time dependent,<sup>20</sup> e.g., a compact produced from a flocced slurry will continue to release strain and grow many hours after pressure release. This time-dependent strain-release phenomenon arises because fluid (liquid or air) must flow into the compact to allow the compressed particle network to grow and relieve its stored strain. Release of the applied pressure will cause the fluid within the compact to share the stored network strain and thus place the fluid in tension. Fluid flow after pressure release is driven by the negative fluid pressure within the compact relative to the ambient pressure outside the compact. Because the fluid must flow from the surface to the interior, the strain within the compact is not uniformly released; i.e., strain is first released from the surface of the body.

In practice, strain is likely to be relieved first at one region on the surface. The

growth of this region during strain release will be constrained by the rest of the body, and it will produce tensile stress similar to an inclusion. These tensile stresses can produce radial cracks. Cracks are more frequently observed at higher filtration pressures where more stored strain is released. As detailed elsewhere,<sup>20</sup> cracking after pressure filtration can be avoided by increasing the resistance of the compact to crack growth, e.g., by adding small amounts (<2 wt%) of certain polymers to the slurry, which apparently bonds the particles as they form the consolidated layer during pressure filtration.

Figure 8(B) also illustrates that bodies formed with dispersed slurries relieve their stored strain within a much shorter period relative to bodies formed with flocced slurries. The reason is that the body formed with the dispersed slurry is still a fluid after pressure filtration, albeit, with a higher viscosity relative to the initial slurry. That is, the consolidated body itself can flow to release stored strain after filtration. Bodies formed from dispersed slurries will continue to flow after removal from their die cavities, much like "silly putty," which has similar dilatant rheology.

Pressure filtration is not the only method to fractionate particles from slurries to form a shape. Centrifugation of flocced slurries can accomplish the same task and avoids the mass segregation produced by centrifuging dispersed slurries.<sup>14</sup> Although it is not as well developed as pressure filtration, with innovative design, centrifugation offers great potential in shaping colloiddally prepared powders.

## V. Densification

Powder compacts are densified at temperatures where mass transport eliminates the void phase. Mass transport is driven by the excess free energy associated with the surface area of the powder. The difference in surface curvature where the particles touch (net negative curvature), relative to the rest of the surface of the particle (positive curvature), causes mass to "fill" the contact region between touching particles. This process is called sintering. If mass is removed from between particle centers, mass transport will lead to shrinkage and densification. If the particles are crystals, a grain boundary forms and grows as sintering proceeds. In considering the free energy change of a powder compact, the increased energy associated with growing grain boundaries must be taken into account as well as the decrease in particle surface energy. With this thermodynamic consideration, one can show<sup>29</sup> that sintering will stop, i.e., mass transport to form a neck between touching particles terminates, when

$$-dA_S/dA_B = \gamma_B/\gamma_S \quad (3)$$

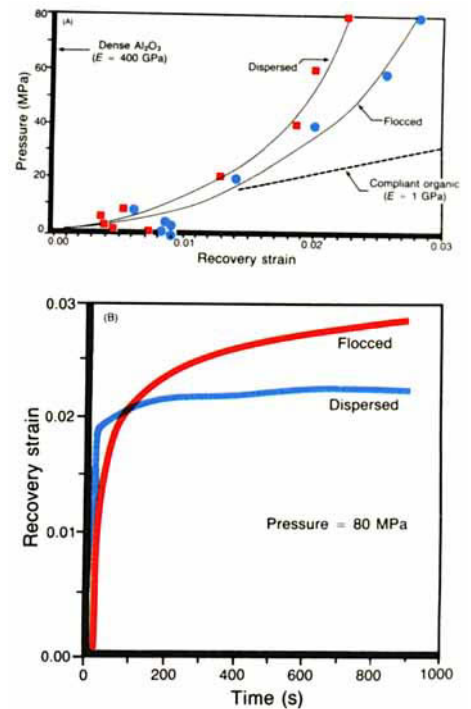


Fig. 8. (A) Elastic strain recovered after different saturated  $\text{Al}_2\text{O}_3$  powder bodies were consolidated from either dispersed or flocced slurries by pressure filtration at different applied pressures. Note that the nonlinear stress-strain relation is similar to that expected from Hertzian elastic behavior, viz.,  $\sigma = B\varepsilon^{3/2}$ .<sup>20</sup> (B) Time-dependent strain recovered after pressure filtration (80 MPa) of dispersed and flocced  $\text{Al}_2\text{O}_3$  slurries.<sup>20</sup> Note that the recovery period for the body formed with the flocced slurry is much longer.

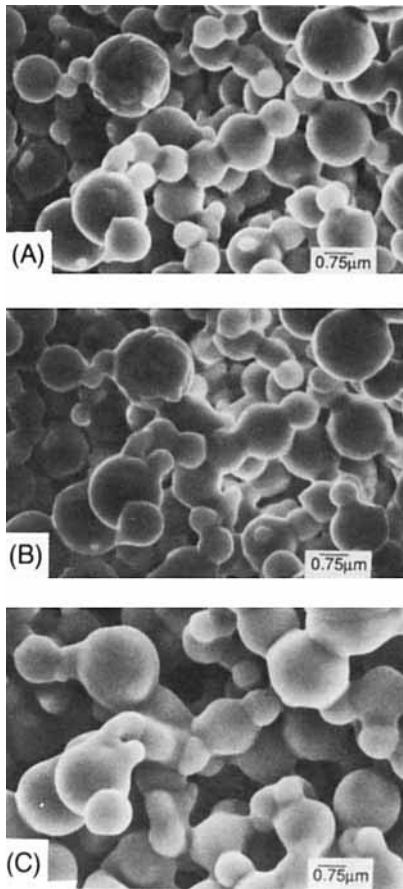


Fig. 9. Micrographs of spherical  $ZrO_2$  (+ 8 mol%  $Y_2O_3$ ) particles produced by electrostatic atomization of zirconia acetate: (A) after sintering by heating to  $1300^\circ C$  for 10 h, (B) same area after further heat treatment at  $1300^\circ C$  for 18 h, and (C)  $1400^\circ C$  for 4 h, where similar network has undergone coarsening and further densification.<sup>31</sup>

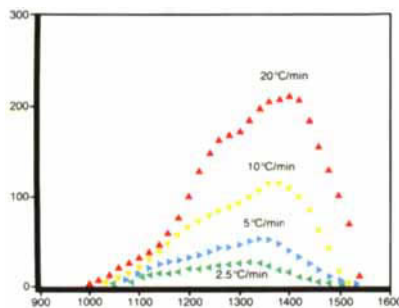


Fig. 10. Shrinkage strain rate versus temperature for identical  $Al_2O_3$  compacts heated to  $1500^\circ C$  at different heating rates. Maximum strain rate occurred at a relative density of 0.77 for all three specimens.

where  $dA_s$  is the change in surface area,  $dA_b$  is the change in grain-boundary area, and  $\gamma_b$  and  $\gamma_s$  are the energy per area associated with grain boundaries and particle surfaces, respectively.

When a linear array of touching particles sinter, they form an equilibrium configuration which satisfies Eq. (3). If mass is removed from between particle centers, the shrinkage of the linear array can be predicted with knowledge of  $\gamma_b/\gamma_s$ . Although the linear array can be used to estimate shrinkage during sintering, it does not enclose and define a void space and thus cannot be used to fully understand and predict the disappearance of pores within powder compacts.

The void space within a powder compact can be structurally defined as pores, which are defined by irregular polyhedra of touching particles connected to one another to form the particle network.<sup>30</sup> Each polyhedron contains one pore. The number of touching particles surrounding and defining each pore is called the coordination number of the pore ( $n$ ) (equivalent to the number of vertices that define each polyhedron). The question is whether or not sintering can eliminate each and every pore defined by the connective network of different polyhedra.

To answer this question Kellett and Lange<sup>29</sup> used Eq. (3) to analytically determine the sintered, equilibrium configuration of different regular polyhedra formed with identical, touching spherical particles. It was shown that pores within all polyhedra shrink (decrease their volume) during sintering, but only pores with a coordination number less than a critical value ( $n \leq n_c$ ) disappear. Pores with  $n > n_c$  shrink to an equilibrium size. The critical coordination number is related to the ratio,  $\gamma_b/\gamma_s$ ;<sup>29</sup> the greater  $\gamma_b/\gamma_s$ , the greater  $n_c$ . It was therefore concluded that all pores within a powder compact will shrink during sintering, but not all would disappear; i.e., sintering alone may not result in full densification.

The sintered network of touching  $ZrO_2$  spherical particles developed by heating at  $1300^\circ C$  for 10 h is shown in Fig. 9(A). Note in Figs. 9(B) and (C) that when the same area is viewed after a subsequent heat treatment at  $1300^\circ C$  for 18 h and  $1400^\circ C$  for 4 h, respectively, the particle network appears similar. The micrographs show differences. First, smaller particles (or grains) have become either smaller or disappear, whereas larger particles become larger, i.e., coarsening has occurred. Second, groups of grains rearranged relative to others. Third, measurements show that some shrinkage, i.e., densification, occurred. Fourth, very few new contacts are made. The more comprehensive study<sup>31</sup> from which these micrographs are taken show that once the initially touching particles sinter to form a metastable network, further densification is related to grain coarsening,

which continuously alters the network configuration.

Although mass transport to the contact region may stop when Eq. (3) is satisfied, adjacent sintered grains will have different radii of curvature that will drive interparticle mass transport. Interparticle mass transport will cause coarsening; i.e., smaller grains disappear as larger grains grow. It can be shown that the decrease in free energy for interparticle mass transport is much smaller than the decrease associated with transport to the contact region. That is, the differential curvature between two particles is much smaller than the differential between particles and their contact region. In addition, during coarsening, the grains become larger. Larger grains result in larger radii and a lower driving force for interparticle mass transport. Thus, one might expect the kinetics for interparticle mass transport leading to coarsening (grain growth) to be slower than the transport to the contact regions (sintering).

If we argue that rapid transport to the contact region leads to shrinkage by sintering and the development of a metastable network similar to that shown in Fig. 9(A) and that further shrinkage is controlled by slower interparticle transport, then the kinetics of densification should be separated by two regimes: an initial regime controlled by sintering kinetics and a subsequent regime controlled by coarsening kinetics. Because the sintering regime results in shrinkage to a metastable network with a given relative density, further densification must be controlled by coarsening kinetics. Thus, the two regimes will be separated by the relative density of the metastable network produced by sintering.

Figure 10 shows the shrinkage strain rate determined when different specimens cut from a single powder compact of  $Al_2O_3$  were heated to  $1550^\circ C$  at different heating rates.<sup>32</sup> In each case, the shrinkage strain rate increases to a maximum and then decreases. The maximum shrinkage strain rate corresponds to the inflection in relative density versus temperature curves commonly obtained in densification experiments. For each curve, the maximum shrinkage strain rate occurs at the same relative density of 0.77. These data strongly suggest that sintering kinetics dominate up to a relative density of 0.77, where coarsening kinetics dominate during further densification.

The question of how coarsening phenomena are related to the thermodynamics of pore stability can be viewed in two different, but complementary, ways. First, it can be seen that coarsening will decrease the coordination number of stable pores, i.e., convert a stable pore with  $n < n_c$  to an unstable pore with  $n \leq n_c$ . Kellett and Lange<sup>33</sup> have shown that isolated pores produced

in a powder compact when polymer spheres pyrolyze during heating will only disappear when grain growth decreases their coordination number below a critical value.

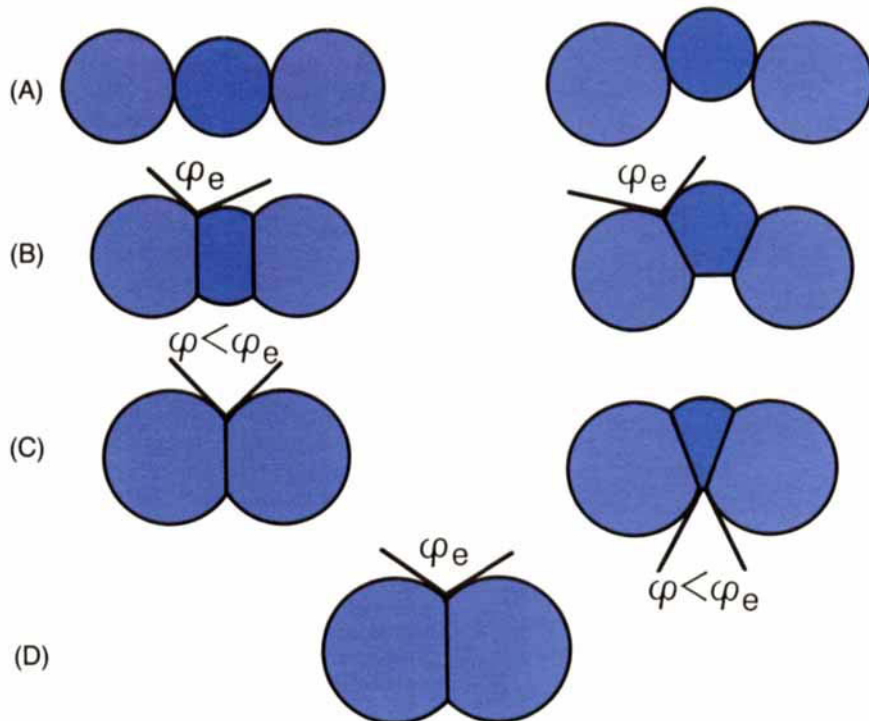
Second, the relation among coarsening, configurational changes in the network during coarsening, and shrinkage can be obtained by examining what happens when grains disappear within a sintered network. Figure 11(A) illustrates three truncated, spherical particles taken from a network which has shrunk to a metastable configuration by sintering. The dihedral angle  $\varphi_e$  defines the equilibrium between the surface and grain-boundary energies which will be achieved when Eq. (3) is satisfied, viz.,  $2 \cos(\varphi_e/2) = \gamma_b/\gamma_s$ . As coarsening proceeds, the smaller grain becomes smaller and the neighboring grains become larger while  $\varphi_e$  is maintained wherever the grain boundary intersects the surface. At some point during coarsening, the neighboring grains touch one another as illustrated in Fig. 11(C). It can be shown<sup>34</sup> that when the neighboring grains touch, the angle formed by the surface tangents and the new grain boundary is less than  $\varphi_e$ . Because  $\varphi < \varphi_e$ , mass transport to the contact region, i.e., sintering, will reinitiate. Contrary to intuition, it can also be shown<sup>34</sup> that very little shrinkage occurs as the smaller particle disappears; i.e., for pertinent values of  $\gamma_b/\gamma_s$ , the larger particles grow at the same rate that the smaller one shrinks. Once the larger particles touch one another, shrinkage occurs by the reinitiation of sintering until a new metastable configuration develops that satisfies Eq. (3) as shown in Fig. 11(D). Thus, although most of the mass transport period is consumed by coarsening, coarsening reinitiates sintering and shrinkage. At the same time, coarsening decreases the pore coordination number.

The amount of grain growth (coarsening) required to fully densify a powder compact after the initial stage of sintering depends on the coordination number distribution of pores within the compact. Compacts where all pores have  $n \leq n_c$  require no grain growth; for this case, all pores disappear during the initial stage of sintering. A predictive relation between grain growth, relative density, and pore coordination number distribution does exist,<sup>34</sup> and it mimics the experimental relation reported by Gupta for a variety of different powder compacts.<sup>35</sup>

It can also be imagined that a major role of applied pressure during densification (hot-pressing, hot-gas isopressing) is to deform the sintering network to form new particle contacts which are infrequently formed during pressureless sintering. Forming new particle contacts via deformation decreases the need for coarsening.

This discussion illustrates how particle packing influences both the ther-

modynamics and kinetics of densification. The ultimate objective is to form a powder compact where all pores are defined by  $n \leq n_c$ . Methods for achieving this packing arrangement are still controversial. The periodic packing of identical particles has been suggested as one means to achieve this objective.<sup>36</sup> Unfortunately, it appears that periodic packing is limit-



ed to small domains which produce a granular periodic packing arrangement much like the granular microstructure of polycrystals. Figure 12 illustrates the problem that can arise when such a periodic, granular arrangement is heat-treated, viz., cracklike voids open at domain boundaries. For this reason, some investigators have shifted their attention to the investigation of particle-size distributions that produce high packing densities with disordered arrangements which minimize the volume of pores with  $n > n_c$ .

Today, one must live with and use commercial powders until manufacturers make improved powders available. Using the colloidal approach, such powders can be fractionated to achieve desired particle-size distributions which maximize packing density when one of the colloidal compatible consolidation methods is employed. Although the ultimate goal may not be economically achieved with these powders (all pores with  $n \leq n_c$ ), a secondary goal should be pursued: powder compacts with a uniform, narrow distribution of pore coordination numbers such that the pores that disappear last during the coarsening stage are as closely spaced as possible. This goal does not necessarily require high packing density, but does require packing uniformity. One pore with a very large coordination

Fig. 11. Three particles, in two configurations, which ((A) to (B)) shrink together by sintering and ((B) to (C)) coarsen (center particle shrinks) and then ((C) to (D)) sinter again. Note that the configuration development on the right is observed in the upper left of Fig. 9.

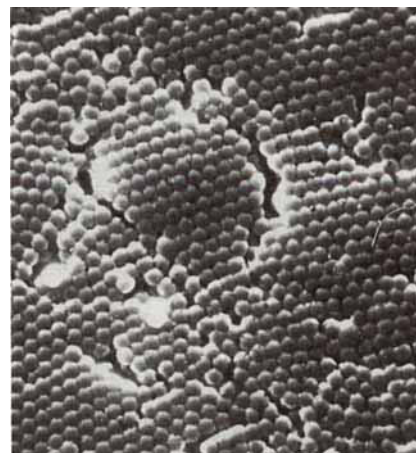


Fig. 12. Partial densification of periodically packed, multilayered arrangement of polymer spheres. Note opening displacements at domain boundaries.

number will not only require extensive grain growth to satisfy its thermodynamics for instability, but its disappearance will also be kinetically limited once it is unstable.

### VI. Control of Grain Growth

The preceding section concluded that some grain growth via coarsening is required to fully densify a powder compact. Although much of this coarsening takes place by the disappearance and growth of adjacent grains through intergranular mass transport, grain boundaries can also move as they would in a fully dense body before full density is achieved. Because matter needs only to diffuse over atomic distances, grain-boundary motion will lead to more rapid grain growth than the coarsening phenomenon. Grain-boundary motion will also trap unstable pores within grains before they have the opportunity to disappear via grain-boundary diffusion. In addition, if a nearly dense body remains at the densification temperature for a short time, grains in many ceramics can grow more than an order of magnitude larger than the average particle size used to form the powder compact. Some grains in ceramics with noncubic crystalline structures can grow to an enormous size relative to their surrounding grains. Although the reasons for abnormal grain growth are still unclear, abnormally large grains can be a dominant, strength-degrading flaw population in many important ceramics. For these and other reasons, grain growth via boundary motion must be controlled to optimize both density and properties.

Second-phase inclusions have become increasingly important in controlling grain size in ceramics. Inclusions generally give rise to residual stresses because of differential thermal contraction and, therefore, are usually thought of as strength-degrading flaw populations themselves. But, it has been shown, both through experimentation<sup>37</sup> and theory,<sup>38</sup> that, if the inclusions are less than a critical size, their residual stress will not induce microcracking either during cooling from the densification temperature or during subsequent stressing. Inclusions with a size that will not induce microcracking can be used to both control grain growth and engineer new composites for desired properties without the fear of degrading strength. For example, large and/or abnormal grain growth can be prevented by the addition of an appropriate inclusion phase as demonstrated by the dramatic strengthening achieved with additions of SiC to Al<sub>2</sub>O<sub>3</sub>,<sup>39</sup> ZrO<sub>2</sub> to β"-Al<sub>2</sub>O<sub>3</sub>,<sup>40</sup> and Al<sub>2</sub>O<sub>3</sub> to cubic ZrO<sub>2</sub>.<sup>41</sup> In each of these cases, the inclusion phase eliminates the most detrimental flaw population, viz., large and/or abnormal grains.

For ceramics, inclusions used to control grain size can be introduced by mix-

ing two-phase powders, e.g., via the colloidal approach. Namely, the inclusions must be effective in retarding grain growth before the powder compact achieves a relative density >0.9, where rapid grain growth is commonly observed in single-phase materials.<sup>35</sup>

Grains are classified by their size (volume) and polyhedron type, the latter defined by the number of faces.<sup>42</sup> As grains decrease their volume, they progressively and sequentially decrease their number of faces. During grain growth, the number of grains per unit volume decreases; i.e., some grains decrease their volume and disappear. Only tetrahedral-shaped grains disappear. Thus, in modeling the effect of perturbations on grain growth, one need only to model the shrinkage and disappearance of simply shaped, tetrahedral grains. The tetrahedral grain decreases its free energy as it decreases its volume. (Grains with many faces (>14) will decrease their free energy by growing.) The derivative of the free energy with respect to the volume of the grain (the Laplace equation) is proportional to the grain-boundary energy per unit area ( $\gamma_g$ ) and inversely proportional to the radius of curvature ( $r$ ) of its grain boundaries, viz.,  $dE/dV = 2\gamma_g/r$ .  $dE/dV$  has the dimension of stress and is referred to as the driving stress ( $\sigma_d$ ) to decrease the volume of a grain. For the tetrahedral grain, the radius of curvature is positive (grain boundaries are concave when looking from within), and  $r \approx 0.6D_t$ , where  $D_t$  is the diameter (grain size) of the equivalent spherical volume of the tetrahedron. Thus, for the tetrahedron,  $\sigma_d = 3.3\gamma_g/D_t$ .

Zener<sup>43</sup> was the first to explain how inclusions retard grain growth. Zener's concept is visualized by Fig. 13(A), which shows, in two dimensions, how a shrinking tetrahedral grain interacts with spherical inclusions of radius  $R$ .<sup>44</sup> As the shrinking grain encounters the inclusion, an increasing proportion of the boundary area is removed from the grain. When  $N$  inclusions are simultaneously intersected, the maximum amount of grain-boundary area removed is  $N\pi R^2$ , which corresponds to a decrease in free energy of  $N\pi R^2\gamma_b$ . If the grain shrinks further, the grain-boundary area adjacent to the inclusions must bow out as it attempts to break away. This bowing and the fact that the grain boundary regains its area occupied by the inclusion during bowing causes the free energy of the system to increase. Using line tension arguments, Zener showed that, as the grain boundary breaks away, the inclusions exert a maximum restraining "stress,"  $\sigma_r = 0.75\gamma_b/R$ , where  $f$  is the volume fraction of inclusions. Thus, the net driving stress for the grain boundaries of a tetrahedral grain to break away from the inclusions is

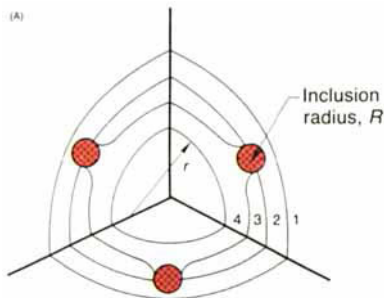


Fig. 13. (A) Two-dimensional schematic of grain boundaries of a tetrahedral grain interacting with spherical inclusions. Different positions illustrate the shape of the boundary as it encounters and breaks away from the inclusions. (B) Energy of the tetrahedral grain versus its volume as it encounters and breaks away from inclusions. Three different curves are for three different retarding stresses produced by inclusions.

$$\sigma_n = \sigma_d - \sigma_r = \gamma_b \left( \frac{3.3}{D_t} - \frac{0.75f}{R} \right) \quad (4)$$

If it is assumed that the kinetics of grain disappearance (growth) are proportional to  $\sigma_n$ , then Eq. (4) shows that inclusions will reduce the kinetics for grain growth.

The free energy versus volume function for inclusion encounter and break away is schematically shown in Fig. 13(B) for the cases where  $\sigma_n > 0$ ,  $\sigma_n = 0$ , and  $\sigma_n < 0$ . The case of  $\sigma_n < 0$  represents the condition ( $f > 4.4R/D_t$ ) where the tetrahedral grain is trapped within a potential well and will not decrease its volume unless thermally activated to "jump out."<sup>44</sup>

Zener's concept and Eq. (4) provide rules for the use of inclusions to hinder grain growth. First, the inclusion must be smaller than the grains. Recent experiments indicate that even when  $f$  is large, inclusions will have no effect on grain growth until their mean grain size is  $>1.5$  times the inclusion size.<sup>45</sup> Second, the smaller the inclusion size, the greater the hindrance to grain growth at a given volume fraction. Third, larger volume fractions will produce greater hindrance. These rules appear to be obeyed for ceramics when the inclusions are immobile, as assumed by the analysis.<sup>45-46</sup> It is still questionable if inclusions will completely prevent grain growth, as suggested for the case where  $\sigma_n < 0$ .

Inclusions can also retard the motion of three- and four-grain junctions. Because it requires much less energy for the inclusion to either break away from a four-grain junction and slip onto a three-grain junction or break away from a three-grain junction and slip onto a two-grain junction (grain boundary) than to break away from a grain boundary and slip into the crystal, inclusions are much more effective in retarding grain growth when they interact with grain boundaries.<sup>44</sup>

The analysis of the preceding paragraph assumes that the inclusions are spatially fixed, i.e., immobile. If the inclusions exhibit sufficient self-diffusion, they can become mobile and can be dragged along by the moving boundaries.<sup>47</sup> Although mobile inclusions can still be effective in retarding grain growth, as Evans<sup>48</sup> has shown for analogous pore drag, they soon coalesce to become larger and less effective. The kinematics of coalescence can be viewed as follows.<sup>44</sup> Mobile inclusions are first collected by moving grain boundaries. Three-grain junctions move together to eliminate grain boundaries and push together inclusions already collected by the disappearing boundary. Finally, four-grain junctions move together to collect all inclusions on three-grain junctions to form a new four-grain junction which contains all collected inclusions. With grain growth, mobile inclusions are relocated to four-grain junctions, their lowest free energy location. During coalescence, inclusions sinter and

undergo grain growth themselves. As grain growth in the major phase proceeds, coalescence of inclusions at four-grain junctions will continue and the ratio of inclusion size to grain size will be maintained constant during further grain growth. Immobile inclusions that effectively retard grain growth at lower temperatures can become mobile at higher temperatures, where they become much less effective because of coalescence.<sup>45</sup>

Because inclusions are introduced into ceramics by mixing powders, their distribution is a critical processing issue. When the inclusions are not uniformly distributed during powder mixing, grain growth in some regions will be less hindered than others. In the extreme case, e.g., where major phase agglomerates are not removed by colloidal fractionation and inclusions cannot be introduced into these agglomerates, the region containing few inclusions will undergo rapid grain growth as shown in Fig. 14. In addition, when very small volume fractions of inclusions are used, their intrinsically poor distribution can exaggerate abnormal grain growth relative to single-phase material.<sup>49</sup> Thus, controlling grain growth with inclusions starts with uniformly prepared powders.

Control of grain growth can also be achieved with minor additions of selected cations which exhibit slight solid solubility.<sup>50</sup> It is usually presumed that these "impurities" will prefer to concentrate at boundaries where they better accommodate the special "crystal chemistries" of grain-boundary structures, i.e., ion-size ratio, charge balance, and coordination number. If the grain boundary were to break away from this planar "cloud of impurities," i.e., if boundary motion were more rapid than the diffusion required to keep the impurities moving with the boundary, then the planar cloud of impurities with area  $A_b$  would now reside within the grain. Grain-boundary break away will increase the free energy by  $dG = \Delta G A_b dD_t$ , where  $\Delta G$  is the free energy per unit volume for the impurity cloud residing within the crystal relative to the boundary and  $dD_t$  is the change in grain size. The restraining stress for the shrinkage of a tetrahedral grain with  $A_b = \alpha D_t^2$  and volume,  $V = \beta D_t^3$ , is  $\sigma_r = dG/dV = (\alpha/3\beta)\Delta G$ , where  $\alpha$  and  $\beta$  are numerical factors.<sup>51</sup> The net driving stress for boundary break away during grain shrinkage is given by

$$\sigma_n = \sigma_d - \sigma_r = \frac{3.3}{D_t} \gamma_b - \frac{\alpha}{3\beta} \Delta G \quad (5)$$

Similar to the case for inclusions, when  $\sigma_n > 0$ , the cloud of impurities will momentarily hinder grain growth, but boundaries can easily break away. With further grain growth, a grain size will be obtained where  $D_t > 10(\alpha/\beta)(\gamma_b/\Delta G)$  and  $\sigma_n < 0$ . Here, the cloud of impurities will severely restrain grain growth and grain growth might be expected to be limited

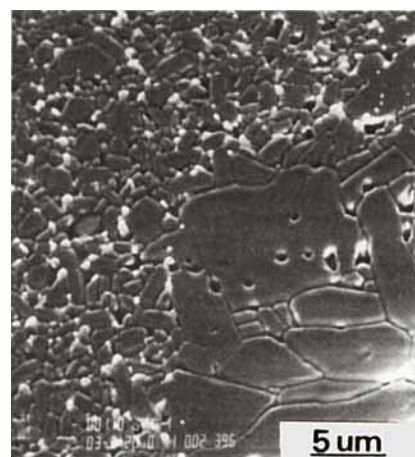


Fig. 14. Micrograph showing that  $ZrO_2$  inclusions (white phase) could not restrain grain growth within  $Al_2O_3$  agglomerate during densification as in surrounding matrix where phases are well mixed.

by the diffusion kinetics of the impurity cloud.<sup>52</sup> Thus, the impurities will have very little effect when the grains are small, but a major effect as the grains grow larger. It is obvious that the greatest effect on grain growth is obtained by choosing impurities that maximize  $\Delta G$ .

The same reasoning has been applied to the case where phase partitioning is concurrent with grain growth. It was observed<sup>53</sup> that grains of the same structure develop different compositions during partitioning. Grain growth in the two-phase compositional region is severely limited relative to single-phase regions but second-phase grains which might hinder grain growth, as discussed earlier in this paper for inclusions, are not observed<sup>53</sup> as initially postulated.<sup>54</sup> If compositional differences between grains did not alter during grain growth (i.e., if boundary motion is faster than the period required to equilibrate compositional gradients), it was reasoned that the boundary would leave behind a "ghost" boundary within the growing grain where the lattice parameters change abruptly because of the compositional gradients. If the compositional gradient between the two grains is a step function, then the ghost boundary would appear as a coherent interface. The different lattice parameters on either side of the ghost boundary would produce a strain energy density,  $U_{se} = K\epsilon^2/E$ , where  $\epsilon$  is the strain due to the change in lattice parameters,  $E$  is the elastic modulus of the material and  $K$  is a dimensionless constant.<sup>53</sup> In the same manner used to develop Eq. (5), the net driving stress for shrinkage of the tetrahedral grain is given by

$$\sigma_n = \sigma_d - \sigma_r = \frac{3.3}{D_t} \gamma_b - K \frac{\epsilon^2}{E} \quad (6)$$

As described for impurity clouds, the grain boundary could easily move to form a ghost boundary when  $D_t$  is small ( $\sigma_n > 0$ ), whereas as grain growth proceeds, a condition will arise ( $D_t > 3.3\gamma_b E/K\epsilon^2$ ) where grain growth will be limited ( $\sigma_n < 0$ ) by the diffusion kinetics required to equilibrate the composition; i.e., grain-growth kinetics will be related to partitioning kinetics. In systems that exhibit extended solid solution, grain-growth control will be more pronounced when small compositional differences produce large differences in lattice parameters.

The use of impurity clouds and phase partitioning to control grain growth is one of accidental discovery due to a lack of understanding of how to systematically choose and engineer compositions that utilize and optimize these important phenomena.

## VII. Concluding Remarks

This review of processing science and technology leading to ceramics with increased reliability suggests certain

research directions. The concepts leading to the colloidal methodology to fractionate and consolidate powders were developed out of a need to eliminate heterogeneities common to powders that produce unwanted flaw populations in structural ceramics.<sup>7</sup> Although the fundamental understanding of interparticle forces is relatively mature, relations between surfactant chemistries and ceramic surface chemistries leading to a predictive choice of surfactants and conditions that optimize and alter interparticle forces consistent with ceramic powder processing is an open research field. Likewise, research leading to a predictive understanding of the slurry rheology as affected by interparticle forces, particulate volume fraction, size, size distribution, and mixed-phase content will significantly aid new ceramic processing technology. Our understanding of powder consolidation mechanics, viz., how particles rearrange during powder flow under conditions of constrained dilatancy, is nonexistent but critical to optimize packing density to optimize densification kinetics. The mechanics of powder compacts themselves, ranging from strain release after consolidation to fracture phenomena, is a research void that must be filled to learn how to consolidate powders from slurries without producing disruptive phenomena. In the past, densification research has emphasized kinetic models of sintering that neglect the effects of particle arrangement. The link between coarsening kinetics and densification kinetics would be one fruitful research topic. Our ability to control grain growth would be greatly enhanced with a fundamental understanding of the effect of impurities on the crystal chemistry of grain-boundary structures and how compositional gradients produced by partitioning effect grain-boundary motion and partitioning kinetics itself. This research would be directed to increase property reliability via increased processing reliability, i.e., processing reliability equals material reliability.

## References

- <sup>1</sup>M. V. Swain, "R-Curve Behavior of Magnesia-Partially-Stabilized Zirconia and its Significance for Thermal Shock"; pp 355-70 in *Fracture Mechanics of Ceramics*, Vol. 5. Edited by R. C. Bradt, A. G. Evans, D. P. H. Hasselman, and F. F. Lange. Plenum Press, New York, 1983.
- <sup>2</sup>D. B. Marshall and A. G. Evans, "Failure Mechanisms in Ceramic-Fiber/Ceramic-Matrix Composites," *J. Am. Ceram. Soc.*, **68** [5] 225-31 (1985).
- <sup>3</sup>F. F. Lange and M. Metcalf, "Processing-Related Fracture Origins: II, Agglomerate Motion and Cracklike Internal Surfaces Caused by Differential Sintering," *J. Am. Ceram. Soc.*, **66** [6] 398-406 (1983).
- <sup>4</sup>R. G. Frey and J. W. Halloran, "Compaction Behavior of Spray-Dried Alumina," *J. Am. Ceram. Soc.*, **67** [3] 199-203 (1984).
- <sup>5</sup>W. H. Rhodes, "Agglomerate and Particle Size Effects on Sintering Ytria-Stabilized Zirconia," *J. Am. Ceram. Soc.*, **64** [1] 19-22 (1981).
- <sup>6</sup>F. F. Lange, "Sinterability of Agglomerated Powders," *J. Am. Ceram. Soc.*, **67** [2] 83-89 (1984).
- <sup>7</sup>F. F. Lange, B. I. Davis, and E. Wright,

"Processing-Related Fracture Origins: IV, Elimination of Voids Produced by Organic Inclusions," *J. Am. Ceram. Soc.*, **69** [1] 66-69 (1986).

<sup>8</sup>V. Engle and H. Hubner, "Strength Improvement of Cemented Carbides by Hot Isostatic Pressing," *J. Mater. Sci.*, **13** [9] 2003-13 (1978).

<sup>9</sup>B. J. Kellett and F. F. Lange, "Experiments on Pore Closure During Hot Isostatic Pressing and Forging," *J. Am. Ceram. Soc.*, **71** [1] 7-12 (1988).

<sup>10</sup>F. F. Lange, "Processing-Related Fracture Origins: I, Observations in Sintered and Isostatically Hot-Pressed  $Al_2O_3/ZrO_2$  Composites," *J. Am. Ceram. Soc.*, **66** [6] 396-98 (1983).

<sup>11</sup>J. W. Goodwin, "The Rheology of Dispersions"; pp. 246-93 in *Colloid Science*, Vol. 2. D. H. Everett (Senior Reporter). The Chemical Society, London, UK, 1975.

<sup>12</sup>M. D. Sacks, "Rheological Science in Ceramic Processing"; pp. 522-38 in *Science of Ceramic Chemical Processing*. Edited by L. L. Hench and D. R. Ulrich. Wiley, New York, 1986.

<sup>13</sup>J. N. Israelachvili, *Intermolecular and Surface Forces*. Academic Press, London, UK, 1985.

<sup>14</sup>F. F. Lange, "Forming a Ceramic by Flocculation and Centrifugal Casting," U.S. Pat. No. 4 624 808, Nov. 25, 1986.

<sup>15</sup>F. F. Lange and M. M. Hirlinger, "Phase Distribution Studies Using Energy Dispersive X-ray Spectral Analysis," *J. Mater. Sci. Lett.*, **4**, 1437-41 (1985).

<sup>16</sup>F. F. Lange and K. T. Miller, "A Colloidal Method to Ensure Phase Homogeneity in  $\beta$ - $Al_2O_3/ZrO_2$  Composite Systems," *J. Am. Ceram. Soc.*, **70** [12] 896-900 (1987).

<sup>17</sup>J. Cesarano III, I. A. Aksay, and A. Bleier, "Stability of Aqueous  $\alpha$ - $Al_2O_3$  Suspensions with Poly(methacrylic acid) Polyelectrolyte," *J. Am. Ceram. Soc.*, **71** [4] 250-55 (1988).

<sup>18</sup>K. P. Darcovich and I. Aksay, "Particle-Sized Distribution of Dense Ceramic Suspensions"; unpublished work.

<sup>19</sup>R. D. Rivers, "Method of Injection Molding Powder Metal Parts," U.S. Pat. No. 4 113 480, Sept. 12, 1978.

<sup>20</sup>F. F. Lange and K. T. Miller, "Pressure Filtration: Kinetics and Mechanics," *Am. Ceram. Soc. Bull.*, **66** [10] 1498-504 (1987).

<sup>21</sup>(a) S. Srijbos, "Pressure Filtration of Permanent Magnetic Powders"; in *Proceedings of the Conference on Hard Magnetic Materials*. Edited by H. Zijlstra. Bond voor Materialenkennis, The Hague, Netherlands, 1974. (b) C. A. M. Van den Broek and A. L. Stuijts, "Ferroxdure," *Philips Tech. Rev.*, **37** [7] 157-75 (1977).

<sup>22</sup>Gebrüder Netzsch, *Maschinenfabrik GmbH and Co.*, Technical Information Bulletin, GK 012, D-8672. Selb, Bavaria, FRG, 1985.

<sup>23</sup>F. M. Tiller and C.-D. Tsai, "Theory of Filtration of Ceramics: I, Slip Casting," *J. Am. Ceram. Soc.*, **69** [12] 882-87 (1986).

<sup>24</sup>J. Dodds and M. Leitselment, "The Relation Between the Structure of Packing Particles and Their Properties"; pp. 56-75 in *Physics of Finely Divided Matter, Procedures in Physics*, Vol. 5. Edited by N. Boccara and M. Daoud. Springer, Berlin, FRG, 1985.

<sup>25</sup>T. J. Fennelly and J. S. Reed, "Mechanics of Pressure Casting," *J. Am. Ceram. Soc.*, **55** [5] 264-68 (1972).

<sup>26</sup>R. A. Davis and H. Deresiewicz, "A Discrete Probabilistic Model for Mechanical Response of a Granular Medium," *Acta Mech. Sin.*, **27**, 69-89 (1977).

<sup>27</sup>S. Timoshenko and J. N. Goodier, *Theory of Elasticity*, 2d ed; pp 372-80. McGraw-Hill, New York, 1951.

<sup>28</sup>K. Walton, "The Effective Elastic Modulus of a Random Packing of Spheres," *J. Mech. Phys. Solids*, **35** [2] 213-26 (1987).

<sup>29</sup>B. J. Kellett and F. F. Lange, "Thermodynamics of Densification: I, Sintering of Simple Particle Arrays, Equilibrium Configurations, Pore Stability, and Shrinkage"; to be published in *J. Am. Ceram. Soc.*

<sup>30</sup>H. J. Frost, "Overview 17: Cavities in Dense Random Packing," *Acta Metall.*, **30** [5] 899-904 (1982).

<sup>31</sup>E. B. Slamovich and F. F. Lange, "Electrostatic Route to Micro-Sized Zirconia Spheres from Liquid Precursors"; Proceedings to be published in *Better Ceramics Through Chemistry III*, MRS Meeting, April 1988.

<sup>32</sup>F. F. Lange; unpublished work.

<sup>33</sup>B. J. Kellett and F. F. Lange, "Thermodynamics of Densification: III, Experimental Relation between Grain Growth and Pore Closure"; unpublished work.

<sup>34</sup>F. F. Lange and B. J. Kellett, "Thermodynamics of Densification: II, Grain Growth in Porous Compact and Relation to Densification," to be published in *J. Am. Ceram. Soc.*

<sup>35</sup>T. K. Gupta, "Possible Correlation Between Density and Grain Size During Sintering," *J. Am. Ceram. Soc.*, **55** [5] 276-77 (1972).

<sup>36</sup>E. A. Barringer and H. K. Bowen, "Synthesis and Processing of Submicrometer Ceramic Powders"; pp. 482-96 in *Science of Ceramic Chemical Processing*. Edited by L. L. Hench and D. R. Ulrich. Wiley, New York, 1986.

<sup>37</sup>D. B. Binns, "Some Physical Properties of Two-Phase Crsytal-Glass Solids"; pp. 315-35 in *Science of Ceramics*. Edited by G. H. Steward. Academic Press, New York, 1962.

<sup>38</sup>D. J. Green, "Microcracking Mechanisms in Ceramics"; p. 457 in *Fracture Mechanics of Ceramics*, Vol. 5. Edited by R. C. Bradt, A. G. Evans, D. P. H. Hasselman, and F. F. Lange. Plenum Press, New York, 1983.

<sup>39</sup>F. F. Lange and M. Claussen, "Some Processing Requirements for Transformation-Toughened Ceramics"; p. 493 in *Ultrastructure Processing of Ceramics, Glasses, and Composites*. Edited by L. L. Hench and D. R. Ulrich. Wiley, New York, 1984.

<sup>40</sup>D. J. Green, "Transformation Toughening and Grain-Size Control in  $\beta$ - $Al_2O_3-ZrO_2$  Composites," *J. Mater. Sci.*, **20** [7] 2639 (1985).

<sup>41</sup>F. J. Esper, K. H. Friese, and H. Geier, "Mechanical, Thermal, and Electrical Properties in the System of Stabilized  $ZrO_2(Y_2O_3)/\alpha$ - $Al_2O_3$ "; pp. 528-36 in *Advances in Ceramics*, Vol. 12, *Science and Technology of Zirconia II*. Edited by N. Claussen, M. Rühle, and A. H. Heuer. American Ceramic Society, Columbus, OH, 1985.

<sup>42</sup>S. K. Kurtz and F. M. A. Carpay, "Microstructure and Normal Grain Growth in Metals and Ceramics: Part I, Theory," *J. Appl. Phys.*, **51** [11] 5725 (1980).

<sup>43</sup>C. Zener, kindly quoted by C. S. Smith, *Trans. Metall. Soc. AIME*, **175**, 15 (1949).

<sup>44</sup>F. F. Lange, "Controlling Grain Growth"; pp. 497-508 in *Ceramic Microstructures '86: Role of Interfaces*. Edited by J. Pask and A. G. Evans, Plenum Press, New York, 1988.

<sup>45</sup>F. F. Lange and M. M. Hirlinger, "Grain Growth in Two-Phase Ceramics:  $Al_2O_3$  Inclusions in  $ZrO_2$ ," *J. Am. Ceram. Soc.*, **70** [11] 827-30 (1987).

<sup>46</sup>D. L. Olgaard and B. Evans, "Effect of Second-Phase Particles on Grain Growth in Calcite," *J. Am. Ceram. Soc.*, **69** [11] C-272-C-277 (1986).

<sup>47</sup>M. F. Ashby and R. M. A. Centamore, "The Dragging of Small Oxide Particles by Migrating Grain Boundaries in Copper," *Acta Metall.*, **16** [9] 1081 (1968).

<sup>48</sup>C. H. Shueh, A. G. Evans, and R. C. Coble, "Microstructural Development During Final/Intermediate Stage Sintering: I, Pore/Grain Boundary Separation," *Acta Metall.*, **30** [7] 1269 (1982).

<sup>49</sup>F. F. Lange and M. M. Hirlinger, "Hindrance of Grain Growth in  $Al_2O_3$  by  $ZrO_2$  Inclusions," *J. Am. Ceram. Soc.*, **67** [3] 164-68 (1984).

<sup>50</sup>S. J. Bennison and M. P. Harmer, "Grain-Growth Kinetics for Alumina in Absence of a Liquid Phase," *J. Am. Ceram. Soc.*, **68** [1] C-22-C-24 (1985).

<sup>51</sup>P. J. Clemm and J. C. Fisher, "The Influence of Grain Boundaries on the Nucleation of Secondary Phases," *Acta Metall.*, **3**, 70-73 (1955).

<sup>52</sup>J. W. Cahn, "Impurity Dray Effect on Grain-Boundary Motion," *Acta Metall.*, **10** [9] 789-98 (1962).

<sup>53</sup>F. F. Lange, D. B. Marshall, and J. R. Porter, "Controlling Microstructure through Phase Partitioning from Metastable Precursors: The  $ZrO_2-Y_2O_3$  System"; pp. 519-32 in *Ultrastructure Processing of Advanced Ceramics*. Edited by J. D. Mackenzie and D. R. Ulrich. Wiley, New York, 1988.

<sup>54</sup>F. F. Lange, "Transformation-Toughened  $ZrO_2$ : Correlations between Grain Size Control and Composition in the System  $ZrO_2-Y_2O_3$ ," *J. Am. Ceram. Soc.*, **69** [3] 240-42 (1986). □